NASA TECHNICAL MEMORANDUM

NASA TM X-68113

NASA TM X-68113

PYROMETER FOR MEASUREMENT OF SURFACE TEMPERATURE DISTRIBUTION ON A ROTATING TURBINE BLADE

by Donald R. Buchele and Daniel J. Lesco
Lewis Research Center
Cleveland, Ohio

TECHNICAL PAPER proposed for presentation at
Symposium on Instrumentation for Airbreathing Propulsion
Monterey, California, September 19-21, 1972

PYROMETER FOR MEASUREMENT OF SURFACE TEMPERATURE DISTRIBUTION ON A ROTATING TURBINE BLADE

by Donald R. Buchele and Daniel J. Lesco

National Aeronautics and Space Administration
Lewis Research Center
Cleveland, Ohio 44135

ABSTRACT

A conceptual optical method and some test results are presented for measuring the surface temperature distribution on one of the rotating turbine bladeswith a surface resolution of 0.05 cm spot diameter at a tip speed of 400 m/sec. The blade is scanned line-by-line by a fixed optical system. During each line-scan, the detector analog output signal is converted to two hundred consecutive digital values that are temporarily stored in a high speed buffer memory, and then transferred at a slower rate to a computer for processing. The signal-to-noise ratio of the silicon avalanche detector is large enough to obtain an accuracy of one percent at 1050K blade temperature. By averaging 25 scans of the same line the same accuracy can be obtained at 900K.

PYROMETER FOR MEASUREMENT OF SURFACE TEMPERATURE DISTRIBUTION ON A ROTATING TURBINE BLADE

by Donald R. Buchele and Daniel J. Lesco

National Aeronautics and Space Administration
Lewis Research Center
Cleveland, Ohio 44135

SUMMARY

A conceptual optical method and some test results are presented for measuring the surface temperature distribution on one of the rotating turbine blades with a surface resolution of 0.05 cm spot diameter at a tip speed of 400 m/sec. The blade is scanned line-by-line by a fixed optical system. The blade moves past a point of focus, generating one line of scan along the blade chord. Scan lines are produced by a row of eighty fibers focused on the blade in a radial direction. The fiber row transmits radiation to a detector that is positioned in front of one fiber at a time, thus scanning the whole blade area. During one line-scan, the detector analog output signal is converted to digital values at a rate of one million conversions per second. Two hundred consecutive digital outputs, representing data for about a 7.5 cm length, are stored in a high speed serial memory. In preparation for the succeeding line-scan, this data is transferred to a computer for processing, averaging, or display. The signal-to-noise ratio of the silicon avalanche detector is large enough to obtain an accuracy of one percent at 1050K blade temperature. By averaging 25 scans of the same line the same accuracy can be obtained at 900K.

INTRODUCTION

Jet engine performance is closely linked to the maximum operating temperature of the turbine blade material. When a blade is constructed

with internal blade passages and surface perforations for the flow of cooling fluids, the surface temperature distribution can show significant changes over a distance less than one millimeter. Temperature changes within this distance can be located and measured by optical imaging of the blade surface--this is impractical with thermocouples. However, an optical method has these problem areas:

1. Install the optical probe in the engine where it can view the blade surface.

2. Protect the probe viewing-window from surface deposits.

3. Obtain sufficient radiation for measurement of a small area on a moving blade.

4. Record and process a large number of measurements that represent temperature distribution over the blade surface.

5. Relate the observed radiation to blade temperature. This is affected by: (a) emittance of the viewed surface; (b) radiation of nearby hot surfaces, gases, and carbon particles, that is reflected from the viewed surface; and (c) gas and particle absorption and emission in the line of sight.

This article will present reasons for the design choices that minimize the problem areas.

This pyrometer is intended for test cell operation where data is generally recorded during steady-state test conditions. Sufficient recording time is available for an optical scanning method to be used. Emphasis is on optical resolution of fine detail on the blade surface and a low blade temperature. The performance desired is:

1. Blade velocity 40,000 cm/sec, and optical resolution of a spot diameter 0.05 cm on blade surface;

2. Temperature range 900 to 1350K with 10K accuracy.

SYMBOLS

c_2	Planck's second radiation constant
D	aperture of probe viewing-lens
f	frequency
L	distance between blade and probe viewing-lens
ℓ	period of sinusoidal temperature distribution
N	radiance of blackbody
S/N	ratio of electrical signal to rms noise
T	blade temperature
v	blade velocity
w	diameter of fiber image on blade
λ	wavelength of radiation
ϕ	radiant flux

OPTICAL SYSTEM

The pyrometer in Fig. 1 contains a fiber optic probe with a row of 80 fibers focused on the blade in a radial direction. Each fiber has an image diameter of 0.05 cm at the blade. In operation, the rotating blade moves past a fixed point of focus, generating a raster of 80 scan lines.

The flexible fiber bundle extends outside the engine to a box where radiation leaving one of the fibers is collected by a microscope and focused on a detector. The microscope views each fiber in sequence by

intermittent advance of the fiber row with an actuator. Thus, the blade area is scanned line-by-line during a time of one to two minutes. A radiation chopper, synchronized and phased to the turbine rotation, intercepts the radiation during one-half of each revolution to provide a dark-input data sample. A shaft-mounted sensor generates a synchronizing pulse to precisely time the blade position and to select one blade for measurement. Radiation from the internal reference lamp is transmitted by three fibers placed in-line with the row of 80 fibers at the fiber-scanning actuator. This lamp provides a correction for drift of the detector response with time. The detector output signal is shown by the waveform in Fig. 2. One-half of the waveform is a dark period when radiation is intercepted by a chopper synchronized and phased to the turbine rotation. The blade scan occupies a fraction of the remaining time. Thus, during the greater part of each revolution, time is available for signal conditioning.

Fiber Optic Probe

A fiber optic probe is preferred to a periscopic lens system because:

1. It can be flexible to simplify installation in the engine.

2. It causes no loss of image resolution of increase of field curvature as it transfers radiation to the detector.

3. It eliminates image vibration by providing a flexible connection between the engine and an external part of the optical system.

4. Individual fibers can be routed as an aid in system design.

In this probe the fibers are adjacent at the viewing lens, and spaced at the actuator for individual viewing by the detector. The spacing prevents radiation reaching the detector from more than one fiber at a time.

The radiation is transferred from a fiber to the detector by a microscope optical system. Lens A in Fig. 1 is focused by lens B as a fixed image on the detector. Lens A accepts radiation from the fiber at F:2.0. A fiber is focused by lens A on B as an image much smaller than B. This provides an allowance for fiber positioning error in the fiber row and by the actuator mechanism.

It is necessary to protect the optical probe and its viewing window from hot gases in the engine. The probe was designed for insertion and removal from a water-cooled tube that was mounted in a blade-viewing position 10 cm downstream from the blade. The tube also provided a gas purge in front of the probe viewing-window, and protected the window from significant surface deposits for several hours.

Wavelength of Measured Radiation

Measurement accuracy is affected by the choice of wavelength. At 900 to 1350K a wavelength of about 1 μm appears to be optimum for the following reasons (refs. 1, 2, and 3):

1. The radiated flux decreases rapidly at a shorter wavelength as given by the Planck function derivative $(dN/N)/(d\lambda/\lambda) = (c_2/\lambda T) - 5$. The quantity on the right is 11 at 1 μm and 900K; the radiance is half as great at a wavelength 5 percent smaller.

2. The fractional error in temperature produced by a fractional error in surface emittance or in flux measurement increases with a longer wavelength as given by the Planck function derivative $(dT/T)/(d\phi/\phi) = \lambda T/c_2$. The quantity on the right is 1/16 at 1 μm and 900K; a 16 percent error in flux measurement corresponds to a 1 percent error in temperature.

3. Extraneous sources of radiation can contribute to the measured flux. At wavelengths 1 μm and shorter, radiation of H_2O, CO_2, and other

molecules becomes small. At wavelengths longer than 0.5 μm, combustor flame chemiluminescence becomes small. (Thermal radiation from nearby hot surfaces and from carbon particles has a spectrum similar to the viewed blade surface. Spectral discrimination is therefore not helpful. This source of error was considered by reference 4.) Extraneous radiation is absorbed at wavelengths less than 0.7 μm by a Wratten filter No. 88A cemented to lens B in Figure 1.

System Performance

The frequency response required for the detector and amplifier depends on the frequency produced by optical scanning. Let the blade have a sinusoidal temperature distribution with period ℓ in the direction of motion. When the blade at a velocity v is scanned, the flux received by the detector has a sinusoidal component with a frequency $f=v/\ell$. The amplitude of the sinusoidal flux component is reduced as its period ℓ becomes small and approximates the diameter w of the fiber image focused on the blade. The amplitude is reduced by a factor of 0.7 when $w \simeq \ell/2$; this gives a frequency of $f \simeq v/2w$ which is the frequency response produced by optical scanning. For $w = 0.05$ cm and $v = 40{,}000$ cm/sec, the frequency f is 400,000 Hz. (Information theory shows the minimum sampling rate is twice per cycle. At a frequency of 400,000 Hz the minimum sampling rate is 800,000 sec^{-1}, and the corresponding sampling distance on the blade is equal to w.) The frequency response of the detector and amplifier should be at least 400,000 Hz to maintain the response produced by the optical scanner.

The accuracy of temperature measurement is limited by the electrical signal/noise ratio of the detector. Tests were made with a silicon avalanche detector and a photomultiplier with S-1 cathode response. The results are presented in two graphs. Figure 3 shows the detector output

signal in terms of blackbody temperature, with no optical system absorption, and a spot diameter $w = 0.05$ cm at the blade, at a distance $L = 10$ cm from a viewing lens of aperture $D = 0.3$ cm. Figure 4 shows the noise and signal/noise ratio in terms of the output signal.

The temperature error caused by the output signal/noise, (S/N), is found using these figures and the Planck function derivative in the form $dT/T = (\lambda T/c_2)(N/S)$ where (N/S) corresponds to a fractional error in flux measurement. The transmission loss of the fiber optic probe is included by reducing the output signal in Fig. 3 by a factor of 0.5. The temperature error is plotted in Fig. 5. This error can be reduced by averaging a number of scans of the same chord line. The noise voltage is divided by the square root of the number of scans; a temperature error of 5 percent at 900K would become 1 percent with 25 scans. The error can also be reduced with a larger fiber and corresponding spot size on the blade. A fiber of twice the diameter would transmit four times the flux, giving four times the signal voltage; the frequency response could be half as great, reducing the noise voltage by $\sqrt{0.5}$. The increased S/N would reduce a temperature error of 5 percent at 900K to 1 percent with one scan.

SIGNAL CONDITIONING ELECTRONICS

To produce a near real-time display of blade surface temperature distribution with the high resolution required, a large amount of high speed data must be rapidly and automatically processed. At the lower end of the temperature range, successive readings of a blade profile must be averaged to enhance S/N ratio. And, of course, the detector

output is a nonlinear function of blade temperature. These criteria emphasize the need for an on-line, dedicated mini-computer to reduce the raw data for an effective display.

Figure 6 is a block diagram of the signal conditioning electronics developed for the measurement system. The detector output is amplified and then fed to a 9-bit (resolution of 1 part in 500) analog-to-digital (A/D) converter. To obtain the desired 0.05 cm surface resolution, the A/D sampling rate must be at least 0.8 MHz. This rapid production of digital data is in excess of allowable computer input rates. Therefore, a data buffer memory in the form of a set of 200-stage shift registers is used. The memory can be loaded with data from the A/D at rates up to 2 MHz. After the 200-point sample has been stored, the data can be shifted out of the memory into a computer at a slower rate. There is sufficient time in one engine revolution for the buffer memory to be unloaded and prepared for the next passage of the test blade.

As an alternate mode of data display, the shift register memory can continuously recirculate a 200-point sample through a digital-to-analog converter for a repetitive analog voltage representation of the raw temperature data which can be displayed on an oscilloscope for study.

The timing and control logic determines when samples should be taken and cycles the buffer memory activity between loading a new sample and recirculating this data.

Amplifier and A/D Converter

The electrical signal output of the silicon avalanche detector is a few millivolts of information together with several hundred millivolts of

DC bias. To amplify the data portion of the output, the amplifier must be AC-coupled so that the large DC bias will not saturate the amplifier. The cyclic dark period signal due to the radiation chopper provides the necessary conversion of input signal to an AC waveform (see fig. 2) for amplification.

The bandwidth of the amplifier is 1 MHz, in keeping with the resolution requirements. The gain can be selected from 250, 500, 1000, and 2000, depending upon the maximum temperature expected, and the calibration curve of the detector (see fig. 3). With a 50 percent flux absorption by the probe, the desired temperature range of 900 to 1350K corresponds to a voltage output range of 0.06 to 8.5 mv. To obtain 1 percent temperature error at 900K, the radiance must be measured to within 16 percent; 16 percent of 0.06 mv is 0.01 mv. If the entire temperature range were to be covered with one gain setting of the linear amplifier, the dynamic range of 0.01 mv to 8.5 mv would require an analog-to-digital converter resolution of about 1 part in 1000 or, in other words, a 10-bit converter. Due to the high cost of high speed converters with this resolution, an 8-bit plus sign converter is used, with the above-mentioned amplifier gain-changing capability used to handle low temperature data.

The 8-bit plus sign A/D converter can operate at conversion rates to 2 MHz. The wide frequency bandwidth makes desirable the use of a 50-Ω input termination; therefore, the amplifier is designed to drive a $\pm$ 5 volt signal into a 50-Ω load.

Buffer Memory

The buffer memory is a set of ten 200-stage recirculating shift registers. This memory must be capable of loading data at the maximum A/D conversion rate of 2 MHz. The use of MOS (metal-oxide-semiconductor) integrated circuit static shift registers fulfills this requirement. The length of memory needed is determined by the number of data points across a blade within one sample. A 200-point memory storing at 2 MHz with a blade velocity of 400 m/sec can hold 200 times 0.02 cm or 4 cm of profile data. Lower conversion rates will increase the profile length proportionately.

The buffer memory stores the A/D converter output bits for each conversion in parallel, and consecutive conversion outputs serially. Between loading new samples, the memory recirculates the data continuously. A synchronizing pulse is available on a separate output to indicate the start of the 200-point grouping. The recirculation frequency is selectable, governed by the computer input interface or the D/A converter maximum operating rate.

Electronics Operation

The system electronics were designed to be compatible with mini-computer capabilities to allow complete system control by a dedicated mini-computer and its associated cathode-ray-tube type of display. It is desirable that a complete turbine blade profile can be obtained with only the manual initiation of a computer program. To allow flexibility in development and check-out procedures, it is also advantageous to provide enough manual control that an operator may position the probe and take

one 200-point sample for indefinite study before continuing. The above-mentioned D/A converter and oscilloscope would be of benefit in this case.

The planned operation of the system for obtaining real-time temperature data under control of a mini-computer is outlined below:

1. Operator initiates computer program.

2. Computer calls for a dark-input data sample. When the chopper is in position, the buffer memory is loaded with a 200-point sample. Upon completion of the sample, the computer is informed that data transfer to the computer can begin. The sample is then averaged in the mini-computer for a dark-input reference.

3. Computer calls for probe radial position 1. When the probe is in position, the computer requests a data sample. A synchronizing pulse from a shaft-mounted sensor triggers the loading of the buffer memory when the test blade enters the view of the probe. When the sample is complete, transfer of the data to the computer memory again takes place. If necessary for data averaging, more samples at probe position 1 can be obtained. The mini-computer then converts the detector voltage data to temperature and prepares the data for transfer to the computer (peripheral) display memory.

4. Step 3 is repeated for all probe positions desired. Various computer techniques for displaying temperature profiles have been developed in the literature. Selection of a technique for this system and development of computer programs to implement the chosen technique are still to be undertaken.

CONCLUSION

The test results presented for the detector and electronic components

satisfy the required pyrometer performance. The optical scanning unit and the fiber optic probe are under construction. The amplifier and buffer memory have been designed and tested. The requirements for the A/D converter were satisfied with a commercially available instrument.

REFERENCES

1. Mossey, P. W.: Experimental Pyrometer for Turbine Blade Temperature Measurement. Paper 690431, SAE, Apr. 1969.

2. Barber, R.: A Radiation Pyrometer Designed for In-Flight Measurement of Turbine Blade Temperatures. Paper 690432, SAE, Apr. 1969.

3. Schilling, B. L.: Methods for Obtaining Surface Temperatures of Material in the Presence of Extraneous Radiation. NASA TN D-4107, 1967.

4. Lowry, William P.; and Gay, Lloyd W.: Errors in Infrared Thermometry and Radiometry. J. Appl. Meteor., vol. 9, Dec. 1970, pp. 929-932.

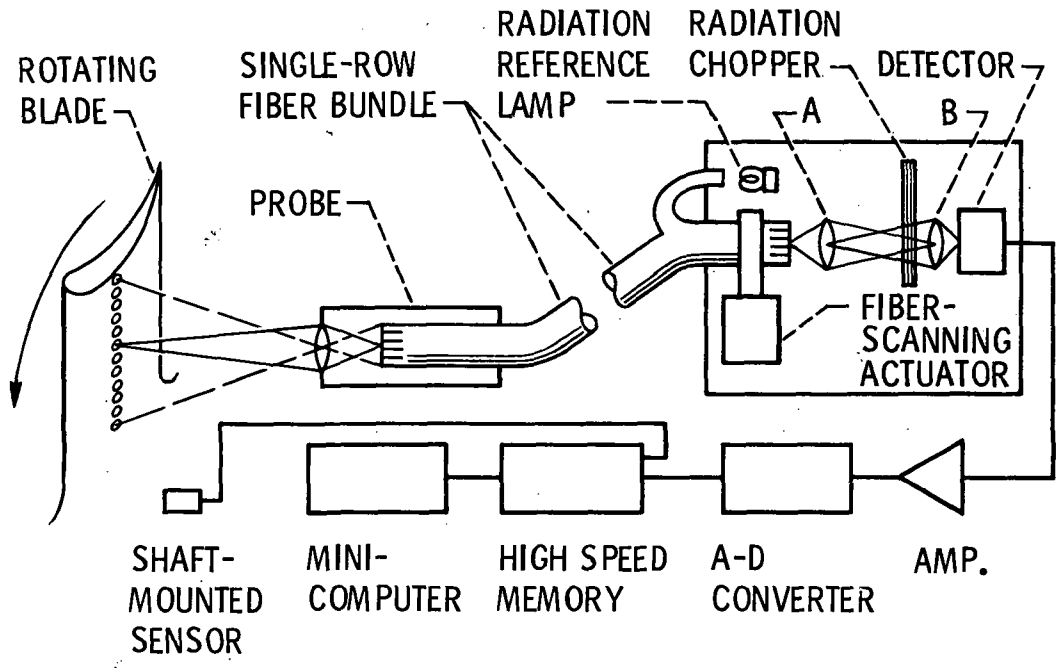

Figure 1. - Turbine blade pyrometer.

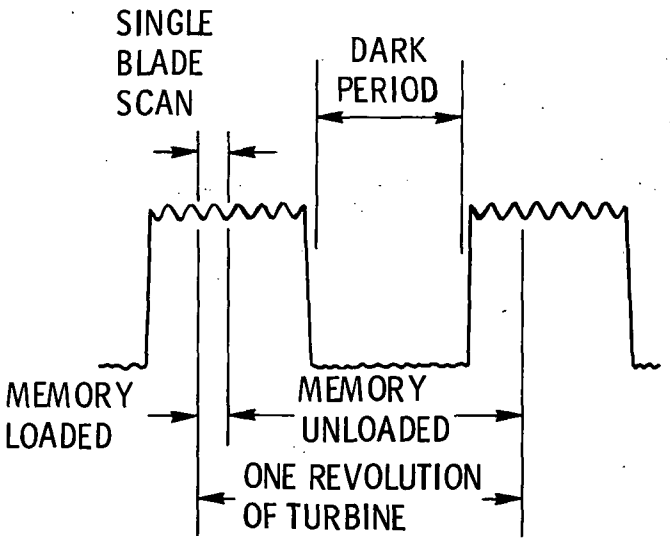

Figure 2. - Detector output waveform.

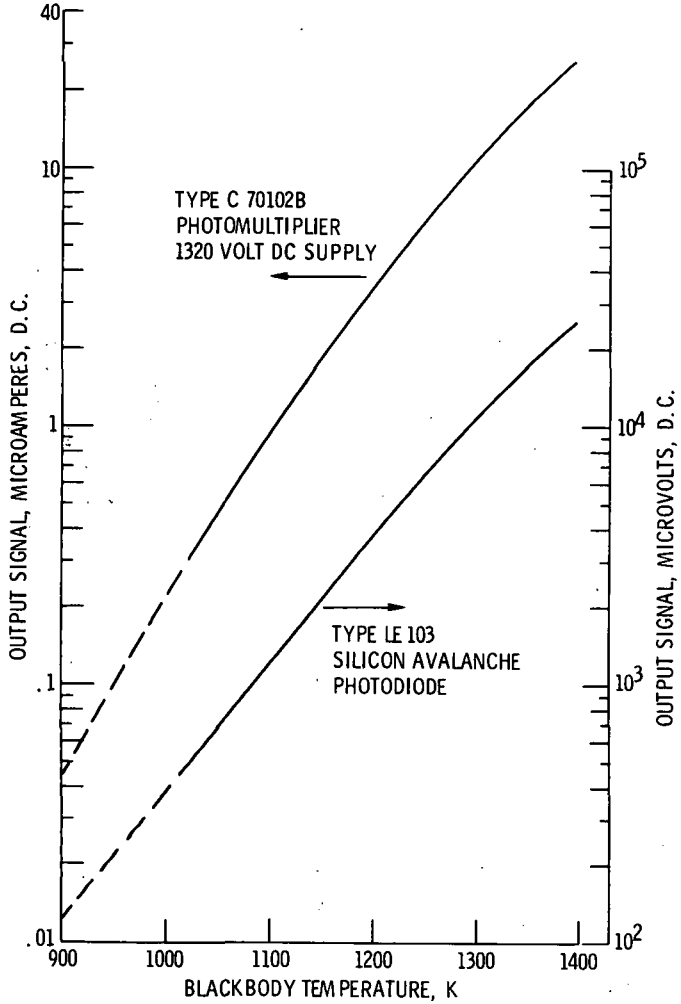

Figure 3. - Detector output signal. Optical throughput geometric factor $(\pi wD/4L)^2 = 1.4 \times 10^{-6}$ cm^2 ster.

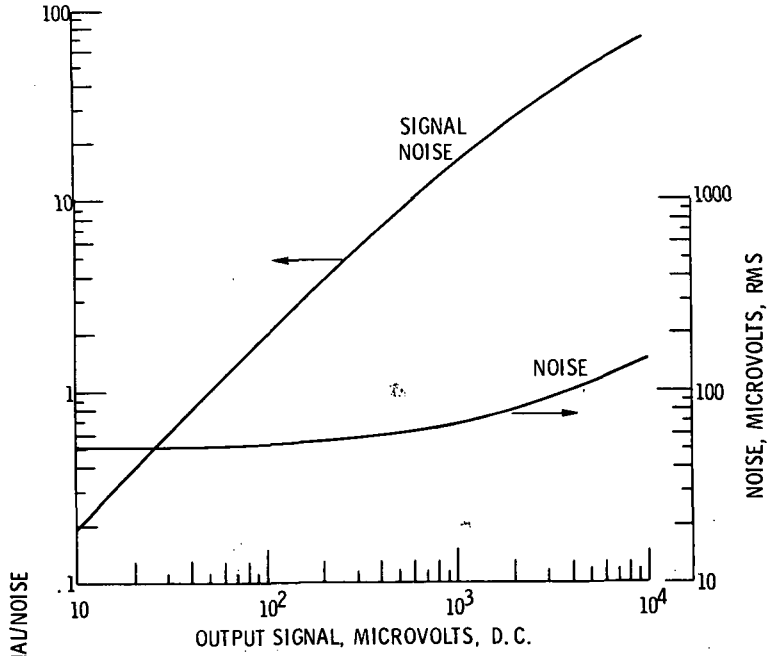

(a) TYPE LE-103 SILICON AVALANCHE PHOTODIODE.

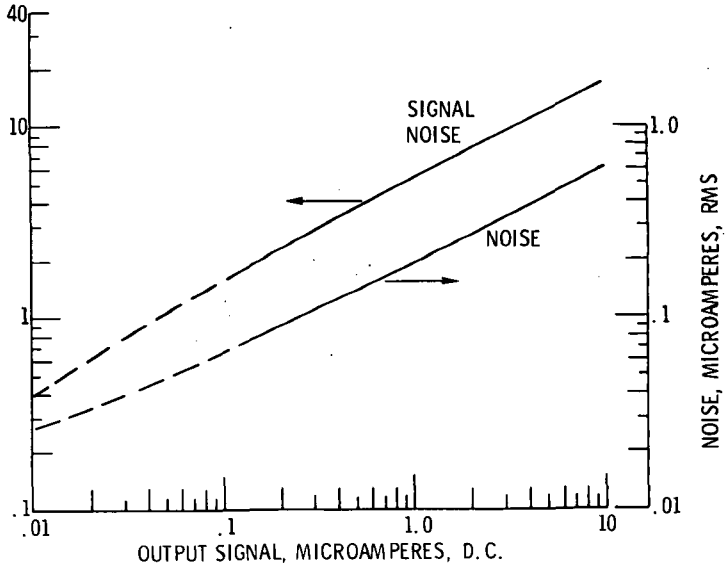

(b) TYPE C 70102B PHOTOMULTIPLIER 1320 VOLT D.C. SUPPLY.

Figure 4. - Detector output at 10^6 Hz bandwidth.

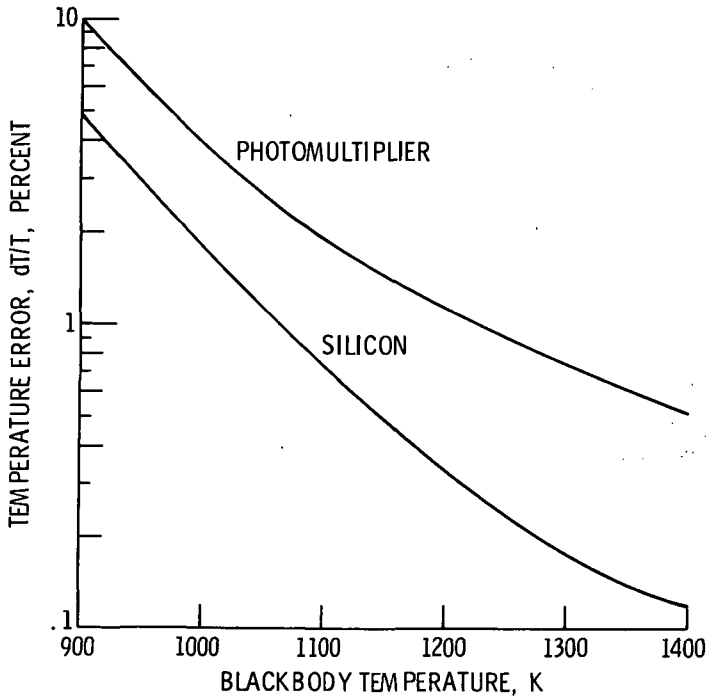

Figure 5. - Blade temperature error caused by detector output noise.

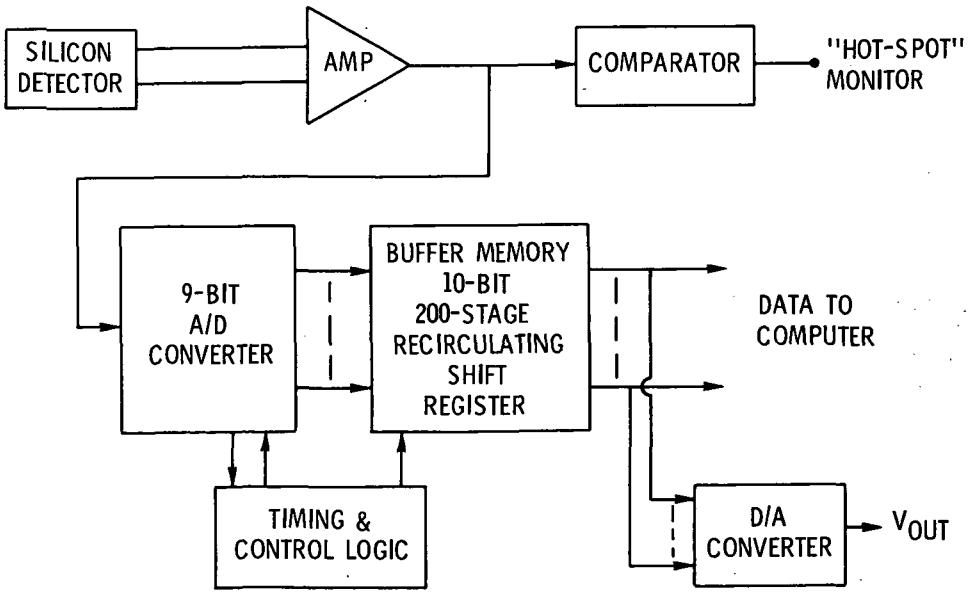

Figure 6. - Block diagram of signal conditioning electronics.